APMA-2017
The 4th International Conference on Powder Metallurgy in Asia
Apr. 09-11, 2017, Hsinchu, Taiwan

Axial Flux PM Machines for compressor application

C. Pompermaier*, J. Washington, L. Sjöberg
[1]Höganäs AB, Höganäs, 263 83, Sweden
*Corresponding author: cristofaro@ieee.org

Abstract **- This paper presents the analysis of an Axial Flux Permanent Magnet (AFPM) Machine with 12 slots, 14 poles applied to a hermetic compressor. The motor is made of Soft Magnetic Composite with NdFeB permanent magnets. The simulations are calculated by 3D Finite Elements Analysis due to the 3D shape of the geometry. Motor performance results are presented including iron loss separation.**

Keywords - 3D machine; Axial Flux Permanent Magnet Machines (AFPM); Soft Magnetic Composites; FEM analysis.

I. Introduction

Soft Magnetic Composite (SMC) materials formed by the powder metallurgy process have isotropic properties in both the mechanical and electromagnetic sense. These materials are formed by coating a powdered iron mix with an electrically insulating non-magnetic material, then pressing the powder into the desired shape. This is a low waste process, allowing complex shapes to be formed that would be prohibitively difficult if a traditional laminated material were used. Some applications of SMC utilising the benefits of the complex shapes and 3D flux carrying capabilities includes Axial Flux Permanent Magnet (AFPM) Machines [1], [2], transverse flux/claw pole machines [3] and linear machines [4]. A recent publication, targets the traction solution for hybrid and full electric vehicles using axial flux permanent magnet machines [5].

When compared to traditional silicon steel laminations, SMC materials have a lower permeability. This is due to the coating and gaps between individual iron particles. This shows up in the B-H curve of the material, implying that if laminations are simply replaced with SMC, with no other design changes the machine will perform poorly by comparison. It is therefore required that the machine is redesigned in such a way as to benefit from the isotopic properties of SMC. By doing so, machines for low cost applications can be targeted [6].

II. Axial Flux Permanent Magnet Machines

The AFPM machine is an attractive substitute to the radial flux machine due to its pancake shape, compact construction and high power density. Because of its short axial length, it is also called a disc-type machine [7].

This topology has the advantage of being very simple to construct by using SMC. AFPM machines may be classified as follows: single-sided, double-sided and multi-stage (multidisc) AFPM machines.

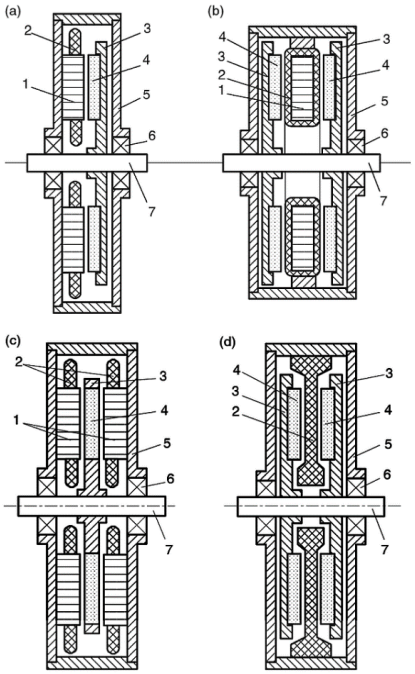


Fig. 1. Basic topologies of AFPM machines: (a) single-sided slotted machine, (b) double-sided slotless machines with internal stator and twin PM rotor, (c) double-sided machine with slotted stator and internal PM rotor, (d) double-sided coreless motor with internal stator. 1 - stator core, 2 - stator winding, 3 - rotor, 4 - PM, 5 - frame, 6 - bearing, 7 - shaft from [7].

For this paper, a three-phase, single-sided AFPM machine topology (Fig. 2) was chosen due to its simplicity. To get a high power density and reduced volume, the configuration of 12 slots and 14 poles (12S14P) is preferred rather than the traditional 12S10P widely used by the industry.

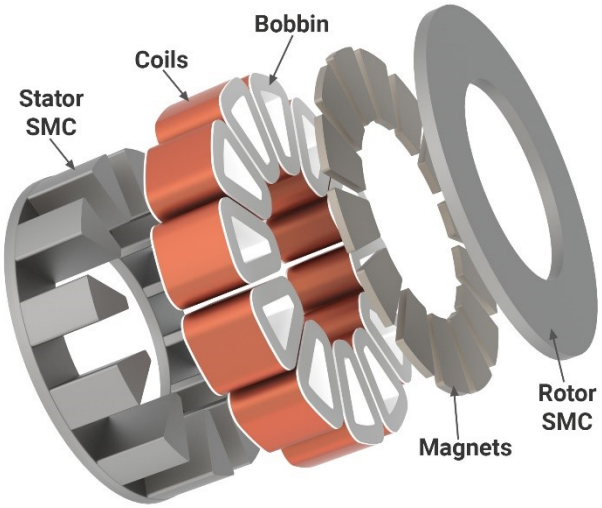


Fig. 2. Exploded view of the AFPM single-sided machine.

III. Hermetic Compressor For Air Conditioning Systems

Hermetic compressor applications demand a duty cycle operation in the range of 50% to 100%. Because of the utilisation factor and the strong competition in this market, compressors demand a high efficiency solution at a low cost.

The AFPM machine has good potential for this application because of its short axial length and the easiness of manufacturing and assembly. Table 1 summarises the application requirements specification for a hermetic compressor. Thus, the study presented in the paper focus on the analysis of an AFPM machine, based on the load condition Envelope point 4, which is the maximum power output.

Table 1. Application requirements specification.

	Speed (rpm)	*Torque (Nm)*	*Power (W)*
Envelope point 1	1200	3.1	310
Envelope point 2	2300	4.8	1156
Envelope point 3	4500	4.9	2309
Envelope point 4	6000	4.0	2513
Rating point 1	1200	1.2	151
Rating point 2	1200	1.7	214
Rating point 3	2300	2.2	530
Rating point 4	4500	2.9	1367
Motor OD (max)	200 mm		
Motor Axial length (max)	50 mm		
Supply voltage	330 V_{DC}		

IV. Finite Elements Analysis

Simulations have been performed with the 3D Finite Element (FE) software Jmag Designer® v15.1. The chosen materials are as presented in Table 2. SMC is used in the rotor coreback to mitigate the joule loss, which would otherwise be significant at high operating frequencies.

The simulations were executed at a temperature of 20 ºC.

Table 2. Motor materials and manufacturers.

Component	*Material*	*Manufacturer*
Stator	Somaloy 700HR 5P 800 Mpa	Höganäs AB
Rotor	Somaloy 700 1P 800 Mpa	Höganäs AB
Magnet	N35SH	Arnold Magnetics
Coil	Copper	-

Fig. 3 shows an example of the mesh selected for the motor 12S14P. It is dense enough to provide accurate results, without taking so long time for the calculations. The total mesh consists of 393886 elements with 82634 nodes (including the air region not shown in the picture).

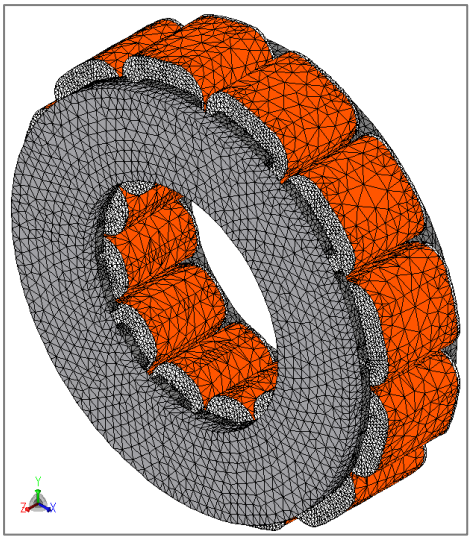


Fig. 3. Mesh view with air mesh suppressed.

Fig. 4 shows the motor with magnets split in four parts to reduce induced joule losses.

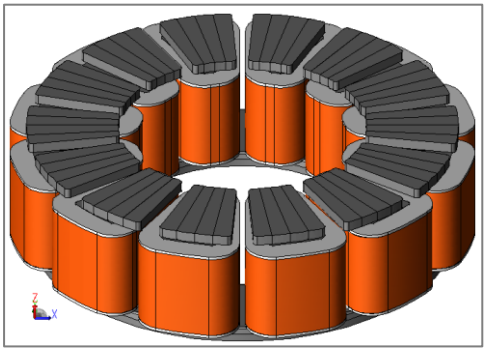


Fig. 4. View of the split magnet in four pieces.

Fig. 5 shows the vectors representing the magnitude of the current density in the coils and

magnets. Note that the current density is minor in the magnets, meaning that the split method is helping to reduce the induced current, and hence the magnet losses.

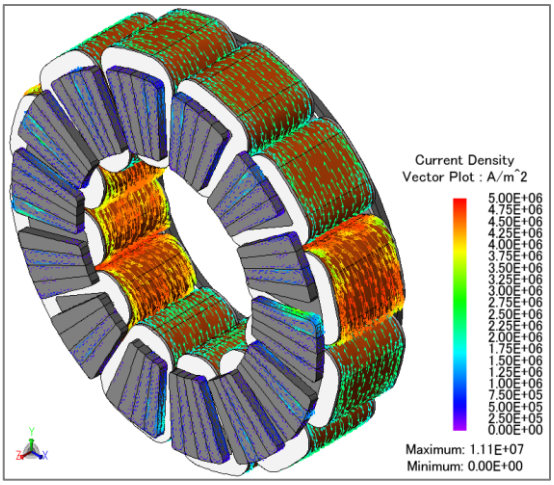


Fig. 5. Current density in the coils and magnets.

Fig. 6 shows the magnetic flux density in the stator. Some small regions in the upper part of the stator teeth is saturated above 1.7 T. Most of the volume of the stator has low flux density, helping to keep the iron loss low.

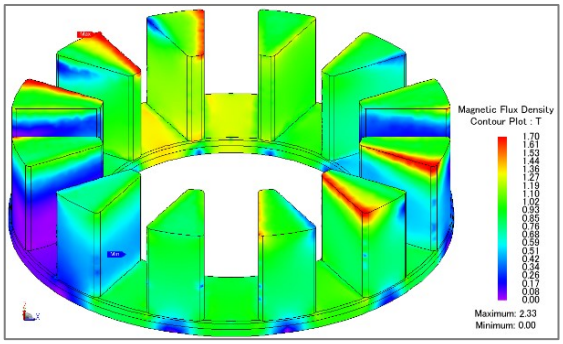


Fig. 6. Magnetic Flux Density in the stator.

V. RESULTS

The total active mass is summarised in Table 3. The total weight is about 1.5 kg, given the output power is 2.6 kW, this machine has the power density of 1.73 kW/kg. In this study, the current density was limited to 5.0 A/mm^2. If more current density were allowed, e.g. 15.0 A/mm^2, the power density would increase to 2.62 kW/kg.

Table 3. Motor active mass summary.

	Per Component	*Total*
Stator SMC (g)	616.32	616.32
Rotor SMC (g)	190.37	190.37
Coil (g)	50.18	602.17
Magnet (g)	6.89	96.42
Motor active mass (g)	-	1505.29

Table 4 outlines the dimensions of the motor. The simulations were performed at no load and rated load condition. Table 5 shows the parameters of the machine.

Table 4. Machine dimensions.

Outer diameter (mm)	120.00
Inner diameter (mm)	53.80
Total Axial Length (mm)	35.60
Air Gap (mm)	1.00
Magnet Span (degree)	140.00
Magnet Depth (mm)	2.60
Rotor Coreback Depth (mm)	4.00
Stator Coreback Depth (mm)	4.00
Stator Tooth Height (mm)	24.00
Coil Width (mm)	5.10
Bobbin Insulation Thickness (mm)	0.75

Table 5. Machine parameters.

Phases	3
Poles	14
Slots (coils)	12
Frequency (Hz)	700
Max Current density (A/mm^2)	5.00
Coil Fill factor	0.67
Wire diameter (bare) (mm)	0.80
Number of strands in parallel	3
Number of turns	51

The results for torque and voltage are shown in Table 6.

Table 6. Torque and voltage summary.

	Parameter	*Value*
No load	**RMS voltage of back EMF (V)**	115.56
	Peak Line-Line Back EMF Voltage (V)	299.31
	Peak Cogging Torque (Nm)	0.07
Rated load	**Average torque @ rated current (Nm)**	4.12
	Torque ripple @ rated current (%)	2.39
	Peak line-line load voltage (V)	299.86

Table 7 shows the inductance at direct and quadrature axis. Note that this AFPM machine has very little saliency.

Table 7. Inductance at direct and quadrature axis.

Inductance Q-axis (mH)	1.91
Inductance D-axis (mH)	1.96

Jmag provides, in the iron loss analysis, the hysteresis and particle losses separately. The losses

are presented in Table 8. Particle losses should not be confused with the bulk joule losses that are dependent on the resistivity of the SMC material and the geometry of the SMC component.

Table 8. Losses at rated load.

	Joule loss (W)	*Iron Loss (W)*	
	Bulk	**Hysteresis**	**Particle**
Stator SMC	3.54	41.22	13.29
Rotor SMC	0.13	4.24	2.24
Magnets	10.80	-	-
Coils	32.36	-	-
TOTAL	46.82	45.45	15.53

Table 9 resumes the performance according to the simulations. The efficiency at the Envelope point 4 in Table 1 is significantly high, reaching 96% neglecting friction and windage losses.

Table 9. Motor performance at rated load.

Current RMS (A)	Speed (rpm)	Total Loss (W)	Torque (Nm)	Pm (W)	Eff (%)
7.54	6000	108	4.12	2591	96

Fig. 7 shows the back EMF at 6000 RPM for one electric period.

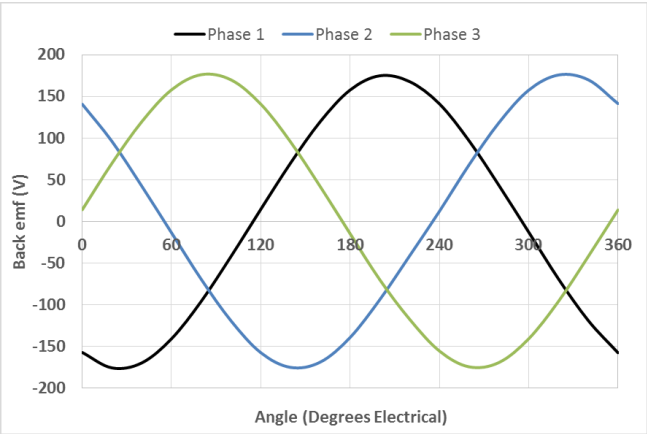


Fig. 7. Back EMF waveform at 6000 RPM.

VI. Conclusion

This paper presented the performance analysis by means of 3D FE of an AFPM machine. The topology shown is suitable for compressor applications because of its compact axial length, high efficiency and ease of assembly in mass production.

The power density can be substantially increased if allowed to use higher current density, which in this study was limited to 5.0 A/mm^2.

Single-sided AFPM machines have similar behaviour to conventional Brushless DC machines, i.e. standard controllers and control techniques can be used.

References

[1] G. Cvetkovski, L. Petkovska, M. Cundev, and S. Gair, "Improved design of a novel PM disk motor by using soft magnetic composite material," *IEEE Trans. Magn.*, vol. 38, no. 5, pp. 3165–3167, 2002.

[2] A. G. Jack, B. C. Mecrow, G. Nord, and P. G. Dickinso, "Axial Flux Motors Using Compacted Insulated Iron Powder and Laminations - Design and Test Results," *IEEE Int. Conf. Electr. Mach. Drives, 2005.*, pp. 378–385, 2005.

[3] J. G. Washington, G. J. Atkinson, N. J. Baker, A. G. Jack, B. C. Mecrow, B. B. Jensen, L. Pennander, G. L. Nord, and L. Sjöberg, "Three-Phase Modulated Pole Machine Topologies Utilizing Mutual Flux Paths," *IEEE Trans. Energy Convers.*, vol. 27, no. 2, pp. 507–515, Jun. 2012.

[4] C. Pompermaier, K. Kalluf, A. Zambonetti, M. V. Ferreira da Luz, and I. Boldea, "Small Linear PM Oscillatory Motor: Magnetic Circuit Modeling Corrected by Axisymmetric 2-D FEM and Experimental Characterization," *IEEE Trans. Ind. Electron.*, vol. 59, no. 3, pp. 1389–1396, Mar. 2012.

[5] O. Maloberti, R. Figueredo, C. Marchand, Y. Choua, D. Condamin, L. Kobylanski, and E. Bomme, "3D-2D Dynamic Magnetic Modeling of an Axial Flux Permanent Magnet Motor With Soft Magnetic Composites for Hybrid Electric Vehicles," *IEEE Trans. Magn.*, vol. 50, no. 6, pp. 1–11, 2014.

[6] C. Liu, J. Zhu, Y. Wang, G. Lei, Y. Guo, and X. Liu, "A low-cost permanent magnet synchorous motor with SMC and ferrite PM," *2014 17th Int. Conf. Electr. Mach. Syst. ICEMS 2014*, pp. 397–400, 2015.

[7] J. F. Gieras, R.-J. Wang, and M. J. Kamper, *Axial Flux Permanent Magnet Brushless Machines*, 2nd ed. Springer, 2008.